Molecular dynamics computer simulation of magnetisation by an electromagnetic field

M.W. Evans [1]

433 Theory Center, Cornell University, Ithaca, NY 14853, USA

Received 19 February 1991; revised manuscript received 14 May 1991; accepted for publication 3 June 1991
Communicated by B. Fricke

The first molecular dynamics computer simulation of magnetisation ($\boldsymbol{M}$) by an electromagnetic field reveals that $\boldsymbol{M}$ has a characteristic dependence on the laser frequency which can be used in principle as a novel kind of non-linear spectroscopy of a variety of useful materials.

1. Introduction

Pershan and coworkers were the first to demonstrate theoretically and experimentally [1–3] the existence of magnetisation ($\boldsymbol{M}$) due to an electromagnetic field, which they named the inverse Faraday effect [4–7]. A peak pulsed ruby laser intensity of about 10^{11} W/m^2 produced bulk magnetisation of the order 0.01 A/m in paramagnetic and diamagnetic samples, respectively a low temperature doped glass and room temperature liquids chosen for their relatively high Verdet constants. The work of Pershan and coworkers remains the only reported experimental investigation of magnetisation by a laser field, and they did not have available in the early sixties the technology to measure the magnetisation as a function of laser frequency, but nevertheless, the inverse Faraday effect has achieved "textbook" status [5,6]. Clearly, the visible frequency pulsed and focused giant ruby laser used in this experimental demonstration sets up a net, coherent, rotational motion of the molecules about its propagation axis, Z, a process which surmounts the energy barriers of diffusional motion in the molecular liquid ensemble at room temperature.

[1] Present address (1990/1991): Institute of Physical Chemistry, University of Zurich, Winterthurerstrasse 190, CH 8057, Zurich, Switzerland.

The theory of the inverse Faraday effect can be developed in terms of the antisymmetric part of the tensor product $E_i E_j^*$ of electric field components of the laser. Here, the symbol E_j^* denotes the complex conjugate of E_j, using tensor subscript notation. The conjugate product is conveniently defined as

$$\Pi_{ij}^{\mathrm{A}} = \tfrac{1}{2}(E_i E_j^* - E_j E_i^*), \quad \Pi_i^{\mathrm{A}} = \epsilon_{ijk}\Pi_{jk}^{\mathrm{A}}, \tag{1}$$

where ϵ_{ijk} is the third rank antisymmetric unit tensor. In this notation, Π_{ij}^{A} is a polar, second rank, antisymmetric tensor, and Π_i^{A} is a rank-one axial tensor, i.e. an axial vector. Both the tensor Π_{ij}^{A} and the vector Π_i^{A} represent the same physical quantity, and are both negative to motion reversal T and parity inversion P. The conjugate product, the optical property responsible for the effect [1–3,8–10], can also be expressed in vector notation by

$$\boldsymbol{\Pi}^{\mathrm{A}} = \boldsymbol{E}_{\mathrm{L}}^{+} \times \boldsymbol{E}_{\mathrm{L}}^{-} = -\boldsymbol{E}_{\mathrm{R}}^{+} \times \boldsymbol{E}_{\mathrm{R}}^{-} = 2E_0^2 \mathrm{i}\boldsymbol{k}, \tag{2}$$

which has the same negative time reversal (T) and positive parity inversion (P) symmetries as static magnetic flux density (B^0 in T). Here $\boldsymbol{E}$ is the electric field strength of the laser in V/m, the subscripts R and L denoting right and left circular polarity and the superscripts the + or − complex conjugates. The unit vector $\boldsymbol{k}$ is taken in the Z axis of the laboratory frame (X, Y, Z) and E_0 is the scalar amplitude (V/m).

In this Letter we report the first molecular dynam-

0375-9601/91/$ 03.50

ics computer simulation of the inverse Faraday effect using the "field applied" technique originally developed [11–14] for static electric fields. The magnetisation by the applied laser is measured in the $t \to \infty$ limit of the angular momentum autocorrelation function along the axis of laser propagation. This shows an intricate dependence on the laser frequency, which indicates the presence of a novel type of laser induced magnetisation spectroscopy of potential utility in a range of materials such as superconductors and composite conducting polymers as well as in the simple illustrative cases explored here for the first time – that of a chiral liquid of D_2 symmetry staggered bicyclopropene molecules and an achiral C_{2v} symmetry water framework. The inverse Faraday effect exists in principle in achiral and chiral ensembles, diamagnetic and paramagnetic. The computer simulation mimicks the experimental demonstration by using a torque set up between an intense, circularly polarised, pump laser, and the appropriate molecular property mediating tensor.

2. The applied torque

The technique of field applied molecular dynamics computer simulation (m.d.) relies on a simple but useful modification [11–14] to the forces loop of any standard m.d. code to add in the torque generated between an applied force field and the appropriate molecular property (the arm of the torque). The particular form of the torque responsible for the inverse Faraday effect is

$$\boldsymbol{T} = -\boldsymbol{m}^{\mathrm{ind}} \times \boldsymbol{B} , \tag{3}$$

where $\boldsymbol{m}^{\mathrm{ind}}$ is a magnetic dipole moment induced by the conjugate product $\boldsymbol{\Pi}^{\mathrm{A}}$ and $\boldsymbol{B}$ is the magnetic component of the applied laser, given in standard IUPAC notation by

$$\begin{aligned}
\boldsymbol{B}_{\mathrm{L}}^{+} &= B_0(\boldsymbol{j} + \mathrm{i}\boldsymbol{i}) \exp(\mathrm{i}\phi_{\mathrm{L}}) , \\
\boldsymbol{B}_{\mathrm{L}}^{-} &= B_0(\boldsymbol{j} - \mathrm{i}\boldsymbol{i}) \exp(-\mathrm{i}\phi_{\mathrm{L}}) , \\
\boldsymbol{B}_{\mathrm{R}}^{+} &= B_0(\boldsymbol{j} - \mathrm{i}\boldsymbol{i}) \exp(\mathrm{i}\phi_{\mathrm{R}}) , \\
\boldsymbol{B}_{\mathrm{R}}^{-} &= B_0(\boldsymbol{j} + \mathrm{i}\boldsymbol{i}) \exp(-\mathrm{i}\phi_{\mathrm{R}}) .
\end{aligned} \tag{4}$$

Integration of the torque (2) over the configuration is the work done, which is minus the potential energy term

$$\Delta H = -\boldsymbol{m}^{\mathrm{ind}} \cdot \boldsymbol{B} , \tag{5}$$

appearing in the interaction Hamiltonian of the inverse Faraday effect. Both the torque and the potential energy are proportional to the product $E_0^2 B_0$, and the induced magnetic dipole moment is proportional to E_0^2. Here E_0 is the scalar electric field strength (V/m) of the pump laser, and B_0 is its scalar magnetic flux density in T.

The induced magnetic dipole moment is given in general by

$$\begin{aligned}
m_1^{\mathrm{ind}} &= -E_0^2 e_{1Z}(b^{\parallel}_{123} - b^{\parallel}_{132}) , \\
m_2^{\mathrm{ind}} &= -E_0^2 e_{2Z}(b^{\parallel}_{213} - b^{\parallel}_{231}) , \\
m_3^{\mathrm{ind}} &= -E_0^2 e_{3Z}(b^{\parallel}_{312} - b^{\parallel}_{321}) ,
\end{aligned} \tag{6}$$

in the molecule fixed frame of reference. Here $\boldsymbol{e}_1$, $\boldsymbol{e}_2$, and $\boldsymbol{e}_3$ are unit vectors in axes 1, 2 and 3 of the principal moment of inertia frame. We have restricted attention here to a D_2 symmetry chiral molecular point group, so that there are only six components of the molecular property tensor b_{ijk} [15–17]. In the C_{2v} point group of water, the symmetry of the tensor $b^{\parallel}_{ijk}$ is coincidentally the same [17], so that numerically the same type of torque suffices in the molecule fixed frame [18] in both cases, with

$$b^{\parallel}_{123} = -b^{\parallel}_{132}, \quad b^{\parallel}_{213} = -b^{\parallel}_{231}, \quad b^{\parallel}_{312} = -b^{\parallel}_{321} . \tag{7}$$

Note that $b^{\parallel}_{ijk}$ is an electronic magnetic electric electric hyperpolarisability, with a well defined quantum structure in matrix density formalism and semi-classical theory. The magnitude of the tensor far from optical resonance has been given by Woźniak et al. [17] to be about 10^{-45} A m^4 V^{-2}, and may increase by several orders of magnitude near optical resonance. These values were arrived at by measurement [17] of the Verdet constant in the conventional Faraday effect to whose mediating tensor $b^{\parallel}_{ijk}$ is closely related by interchange of subscript symmetry. The computer simulation results reported here also show that there is no magnetisation due to the torque set up directly between the $\boldsymbol{E}$ component of the pump laser and the permanent electric dipole moment of water.

3. Computer simulation method

The algorithm is fully described elsewhere [19] and the torque (2) was incorporated as Cartesian components [20] in the force loop, followed by up to 6000 time steps of re-equilibration, each of 5.0 fs for staggered bicylopropene, and 0.5 fs for water. Re-equilibration (rise transient [21]) takes place through a thermostatting routine, which keeps the temperature near the input value until the field-applied statistically stationary state is reached – "field-on equilibrium". In this condition, the molecular dynamics were investigated visually by animation [22]. In field-on equilibrium, time correlation functions were computed by running time averaging [23] over contiguous segments of at least 6000 time steps out to a maximum of 400 time steps, giving good statistics. This procedure was repeated for each Cartesian component of a range of molecular dynamical vectors, including molecular angular momentum ($\boldsymbol{J}$), orientation, net force and torque experienced by a molecule, and center of mass position.

The complete analysis for both molecules was repeated for up to twenty different laser frequencies as a function of $E_0^2 B_0$, the primary objective being the construction of a spectrum of magnetisation as a function of laser frequency in the visible (100 THz) range of available mode locked dye lasers.

A sample of 108 staggered bicyclopropene molecules was used to represent a chiral two bladed propeller, well adapted to respond to a spiralling laser field, and water was used to represent an achiral, diamagnetic, asymmetric top. The chiral intermolecular potential was represented by six Lennard-Jones CH moieties, so that the total intermolecular potential was a six by six Lennard-Jones site–site potential with Lorentz–Berthelot combining rules

$$\frac{\epsilon}{k}(\mathrm{CH}) = 158.0\ \mathrm{K}, \quad \sigma(\mathrm{CH}) = 3.8\ \text{Å}\,. \tag{8}$$

This level of approximation was considered adequate to demonstrate the existence of the phenomenon of frequency dependent magnetisation introduced here. Increased levels of approximation, including ab initio models of the intermolecular potential [24], can be adapted to investigate non-linear phenomena such as the inverse Faraday effect.

The intermolecular potential for water is described fully in the literature [19,25], and is an extended ST2 model fully tested against experimental data [26] and the MCYL ab initio pair potential of Clementi and coworkers [27].

There appear to be no ab initio computations to date of the individual scalar components of the molecular property tensor $b^{\parallel}_{ijk}$ for any atom or molecule, and in consequence, the following relative values were used to compute the torque (2) for both types of molecule

$$b^{\parallel}_{123} : b^{\parallel}_{213} : b^{\parallel}_{312} = 1:2:3\,. \tag{9}$$

The absolute order of magnitude of these elements is given by Woźniak et al. [17].

Data generating runs and computation of time correlation functions were carried out on the IBM 3090-6S supercomputer of ETH Zurich, and video animation on the multi-engine environment designed by Pelkie [22] at Cornell Theory Center's computing environment, following satellite transmission. Video cassettes with narration are available from the author for distribution, giving visual information of great clarity on the development of magnetisation in response to the applied laser field through the torque (2).

4. Results and discussion

Animation analysis revealed visually and directly that in the inverse Faraday effect the laser spins individual molecular properties such as torque, angular momentum, and rotational velocity [19] about its axis of propagation [#1]. This process is always in intricate competition with the Brownian motion, or "background dynamics" [23] when the laser frequency is tuned to the THz range characteristic of visible frequency mode locked lasers. Statistical analysis revealed through time correlation functions that this process depends closely on the applied laser frequency. A data bank was collected of several hundred auto- and cross-correlation functions which

[#1] The animation by C.R. Pelkie from data by M.W. Evans shows the inverse Faraday effect in bromochlorofluoromethane for a variety of dynamical vectors such as angular-momentum, rotational and linear velocity, force, torque, and orientation with scattegram analysis of the statistical effects of the conjugate product of a laser pulse at visible frequencies.

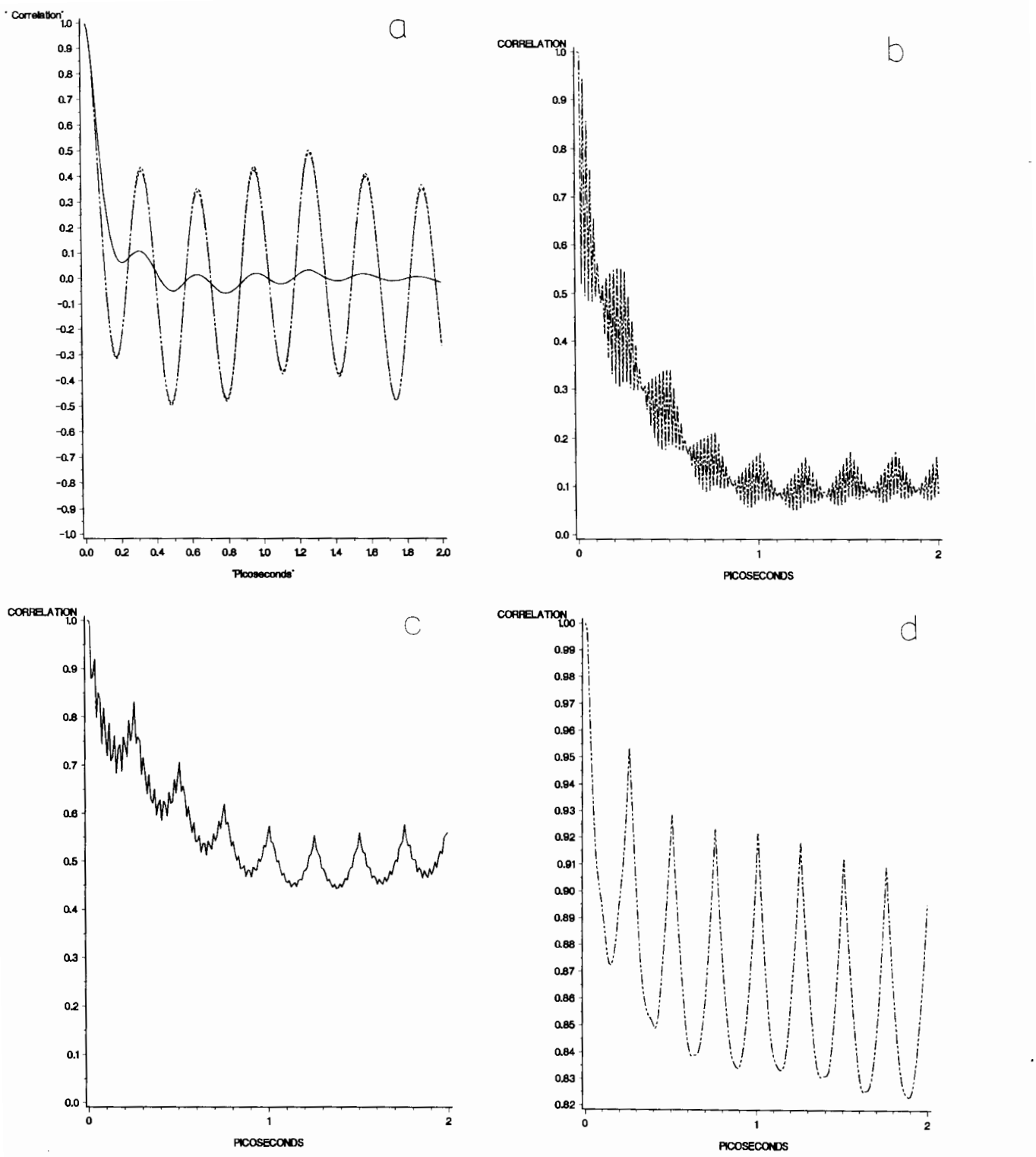

Fig. 1. The angular momentum autocorrelation functions at different laser frequencies for staggered bicyclopropene. The Z component develops a different time dependence from the other two, Z being the axis of laser propagation. (a) 30.0 THz; (b) 450 THz; (c) 600 THz; (d) 840 THz; (e) 1500 THz. (b) to (e) show the Z component only.

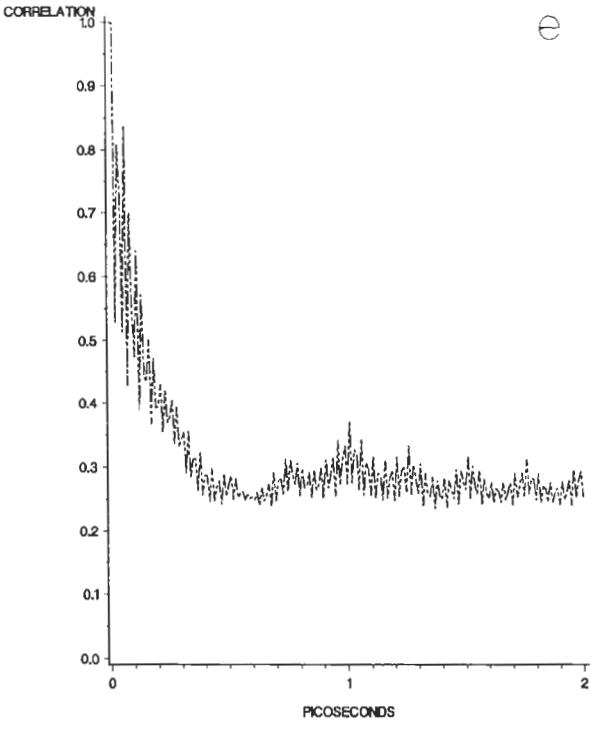

Fig. 1. (continued).

characterise statistically the inverse Faraday effect at up to twenty laser frequencies in the 100 THz range. Of particular significance is the development of a non-vanishing $t\to\infty$ tail (fig. 1) in the angular-momentum autocorrelation function (a.c.f.). The classical molecular angular momentum ($\boldsymbol{J}$) is directly proportional through the gyromagnetic ratio to the molecular magnetic-dipole moment ($\boldsymbol{m}$), and fig. 1 therefore implies the development of a magnetic-dipole moment

$$\boldsymbol{m}_\infty^2 = \frac{\langle m_Z\rangle_{t\to\infty}^2}{\langle m_Z^2\rangle} = \frac{\langle J_Z\rangle_{t\to\infty}^2}{\langle J_Z^2\rangle}\,. \qquad (10)$$

This quantity is recorded against laser frequency in table 1 for several visible frequencies and for both molecules. Table 2 measures the change in internal potential energy brought about by the laser field, and is intended as a guide to the laser intensities used in picosecond pulses in the simulation. (One pulse is equivalent to several thousand time steps in the field applied condition.) The energy pumped into the ensemble by the laser can be worked out from table 2. For example, the energy at 510 THz in staggered bicyclopropene is $-55-(-77)=22$ kJ/mol. Thus the pump laser has given 22 kJ/mol to the liquid, i.e. has *increased* the internal energy of the liquid by about a quarter of its original value. Fig. 2 shows that the permanent magnetic dipole moment is accompanied by the development of orientational cross correlations of the type

Table 1
Magnetisation m_∞^2 versus laser frequency.

Normalised magnetisation	Laser frequency (THz)	Liquid
0.002 ± 0.02	30.0	staggered bicyclopropene
0.025 ± 0.03	300.0	
0.10 ± 0.03	450.0	
0.55 ± 0.02	510.0	
0.67 ± 0.03	540.0	
0.54 ± 0.03	600.0	
0.79 ± 0.03	630.0	
0.76 ± 0.03	660.0	
0.80 ± 0.02	750.0	
0.87 ± 0.05	840.0	
0.80 ± 0.05	900.0	
0.88 ± 0.05	1020.0	
0.80 ± 0.02	1200.0	
0.65 ± 0.02	1350.0	
0.28 ± 0.02	1500.0	
0.00 ± 0.05	1800.0	
0.50 ± 0.02	2400.0	
0.90 ± 0.04	3000.0	
0.05 ± 0.05	300.0	water
0.02 ± 0.07	500.0	
0.02 ± 0.06	600.0	
0.05 ± 0.03	1000.0	

Table 2
Potential energy (kJ/mol) of staggered bicyclopropene.

Energy (kJ/mol)	Laser frequency (THz)
−77	0
−55	510.0
−53	540.0
−63	600.0
−68	750.0
−71	900.0
−59	3000.0

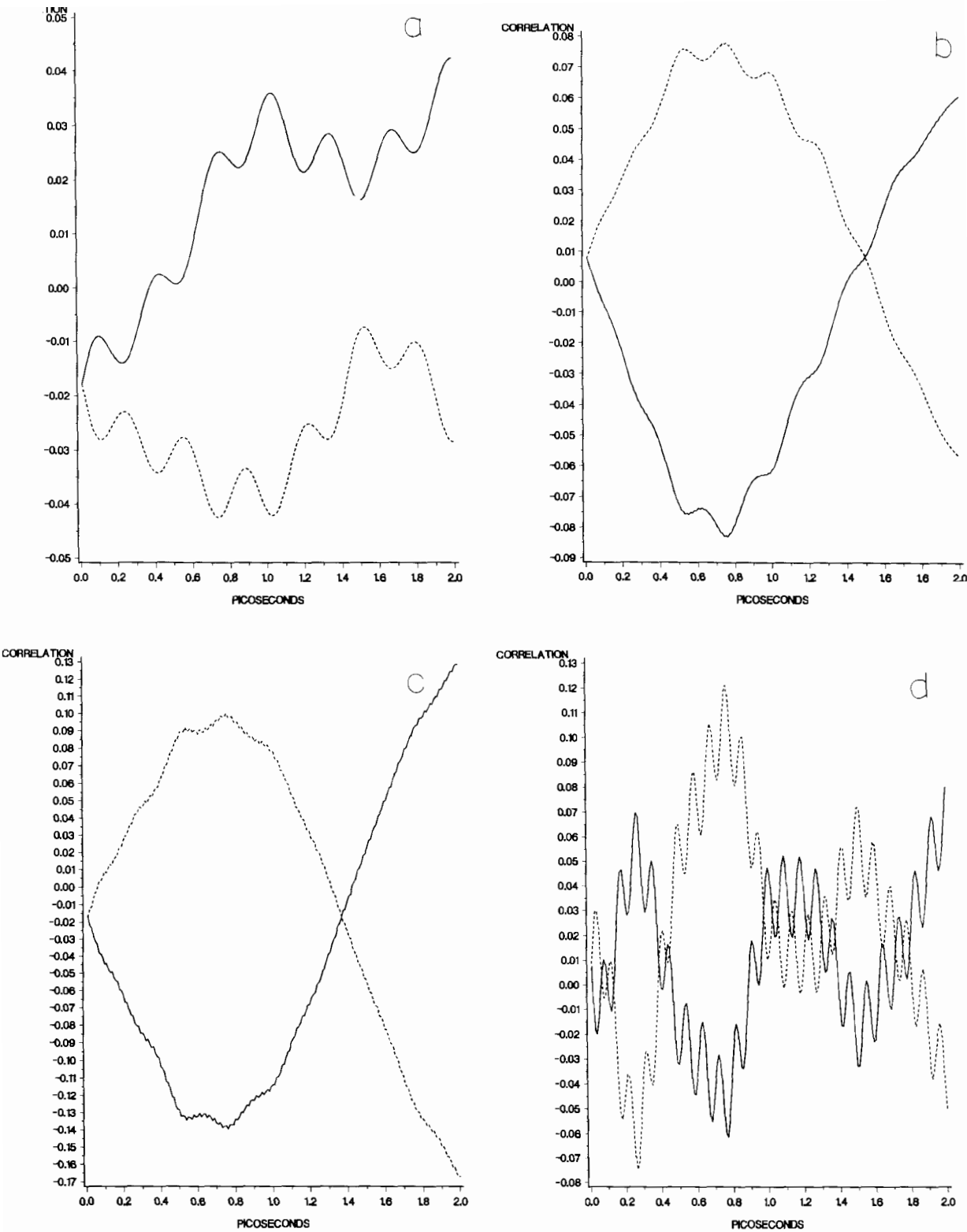

Fig. 2. As for fig. 1, orientational cross correlation functions as defined in eq. (9).

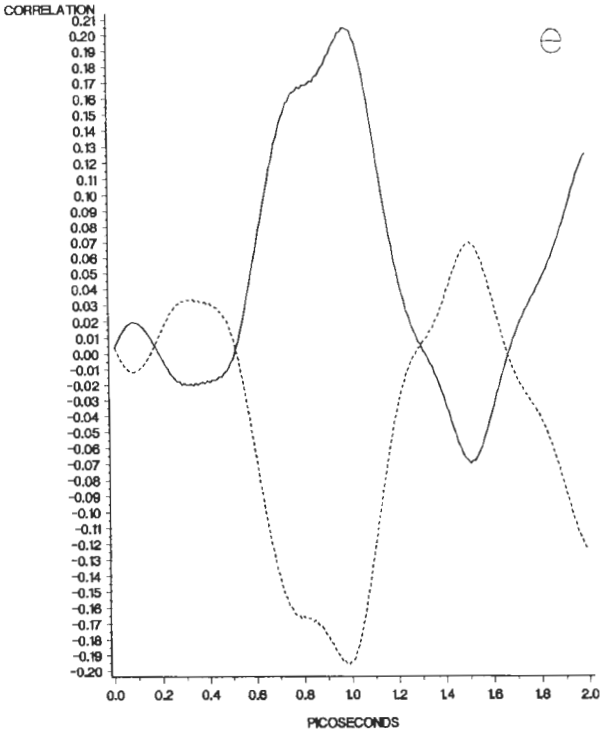

Fig. 2. (continued).

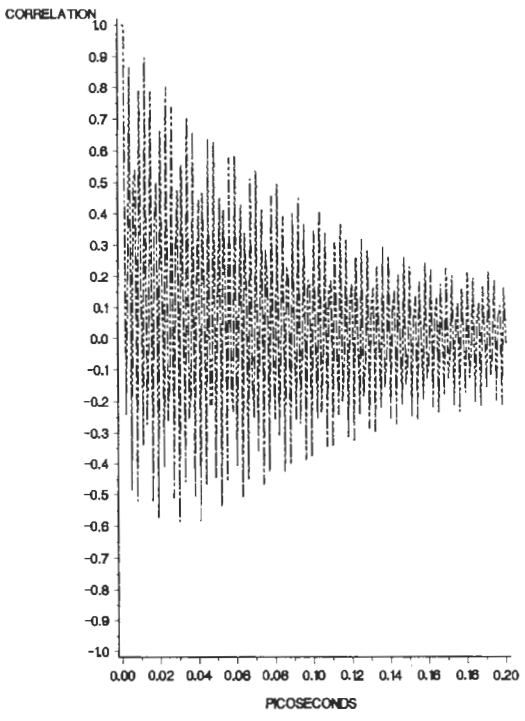

Fig. 3. Z component autocorrelation function in water due to the first order torque, eq. (10), showing that the $t\to\infty$ value vanishes, i.e. there is no magnetisation as in fig. 1.

$$C_1(t)=\frac{\langle e_{1X}(t)e_{1Y}(0)\rangle}{\langle e_{1X}^2\rangle^{1/2}\langle e_{1Y}^2\rangle^{1/2}}$$

$$=-\frac{\langle e_{1Y}(t)e_{1X}(0)\rangle}{\langle e_{1Y}^2\rangle^{1/2}\langle e_{1X}^2\rangle^{1/2}}, \qquad (11)$$

where $\boldsymbol{e}_1$ is a unit vector in an axis of the principal molecular moment of the inertia coordinate system. In fig. 2, five laser frequencies are shown for staggered bicyclopropene, corresponding to those in fig. 1. A similar, intricate, dependence on laser frequency was observed for liquid water, using laser frequencies up to 1000 THz in the visible (mode locked dye laser). The magnetisation m_∞^2 is therefore characteristic of the inverse Faraday effect and its root cause is the frequency independent conjugate product $\boldsymbol{\Pi}^{\mathrm{A}}$. It was checked during the course of this work that the first order torque [28]

$$\boldsymbol{T}_2=-\boldsymbol{\mu}\times\boldsymbol{E} \qquad (12)$$

between the permanent electric dipole moment in water and the electric field component of the pump laser did not produce magnetisation, but rather a result such as illustrated in fig. 3, i.e. a component angular-momentum autocorrelation function which is highly oscillatory and depends on the laser frequency, but which always goes to zero at $t\to\infty$. (Such a check is not needed in staggered bicyclopropene because it is electrically non-dipolar.)

Simulation results for twenty different laser frequencies also showed that the magnetisation m_∞^2 is accompanied by: (i) cross correlation functions between the X and Y components of angular momentum and rotational velocity [19], corresponding to the laser induced spinning motion observed in the animations; (ii) highly oscillatory autocorrelation functions of angular momentum and rotational velocity, in each case the Z component being markedly different from the X and Y components, whose time dependencies were very similar, showing a low "simulation noise" level and "good statistics"; (iii) development of anisotropy in the time dependence of orientational autocorrelation functions, the Z component becoming much longer lived than the other two. The latter was accompanied by the develop-

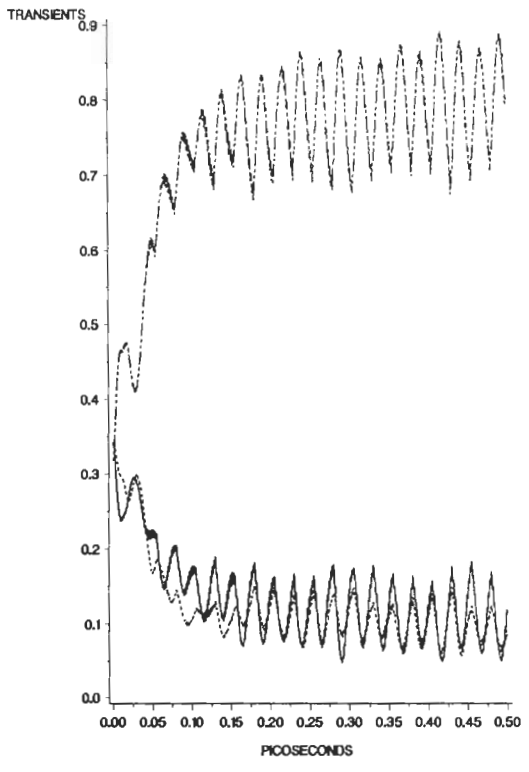

Fig. 4. Second order orientational rise transients in water with a laser applied at $t=0$. The applied laser frequency is 500 THz, corresponding to a wavelength of about 600 nm, in the vicinity of a mode locked rhodamine 6G dye laser in the visible. The upper curve is the transient $\langle e_{1Z}^2 \rangle$, the lower two curves are $\langle e_{1X}^2 \rangle$ and $\langle e_{1Y}^2 \rangle$, showing the development of birefringence due to the inverse Faraday effect.

ment through experimentally accessible [29] sub-picosecond rise transients (fig. 4) of second order orientational averages such as $\langle e_{1Z}^2 \rangle$ in the propagation axis of the laser, where e_1 is a unit vector in a molecular axis such as the 1 axis of the principal molecular moment of the inertia frame of reference. No first order orientational averages were observed. All these characteristics were very sensitive to small changes in the frequency of the laser, as illustrated in figs. 1–3 for a small sample of results.

Acknowledgement

The Swiss NSF is thanked for funding this project, and Professor Georges Wagnière for an invitation. Professors Wagnière and Woźniak are thanked for many interesting discussions. ETH is thanked for a major grant of time on the IBM 3090 and Dr. L.J. Evans for invaluable help with the SAS laser plotting facilities at Irchel. Chris Pelkie is thanked for major animation efforts at Cornell Theory Center.

References

[1] P.S. Pershan, Phys. Rev. 130 (1963) 919.
[2] J.P. van der Ziel, P.S. Pershan and L.D. Malmstrom, Phys. Rev. Lett. 15 (1965) 190.
[3] P.S. Pershan, J.P. van der Ziel and L.D. Malmstrom, Phys. Rev. 143 (1966) 574.
[4] P.W. Atkins and M.H. Miller, Mol. Phys. 15 (1968) 503.
[5] P.W. Atkins, Molecular quantum mechanics (Clarendon, Oxford, 1982).
[6] Y.R. Shen, The principles of non-linear optics (Wiley, New York, 1984).
[7] G. Wagnière, Phys. Rev. A 40 (1989) 2437.
[8] M.W. Evans, Phys. Rev. Lett. 64 (1990) 2909.
[9] M.W. Evans, Opt. Lett. 15 (1990) 863.
[10] M.W. Evans, J. Mod. Opt. 37 (1990) 1655.
[11] M.W. Evans, J. Chem. Phys. 76 (1982) 5473, 5480.
[12] M.W. Evans, J. Chem. Phys. 77 (1982) 4632.
[13] M.W. Evans, J. Chem. Phys. 78 (1983) 925.
[14] M.W. Evans, J. Chem. Phys. 78 (1983) 5403.
[15] S. Kielich, in: Dielectric and related molecular processes, Vol. 1, ed. M. Davies (Chem. Soc., London, 1972).
[16] S. Kielich, Nonlinear molecular optics (Nauka, Moscow, 1981).
[17] S. Woźniak, B. Linder and R. Zawodny, J. Phys. (Paris) 44 (1983) 403.
[18] M.W. Evans, Phys. Rev. A 41 (1990) 4601.
[19] M.W. Evans, in: Advances in chemical physics, Vol. 81, eds. I. Prigogine and S.A. Rice (Wiley–Interscience, New York, 1991), in press [Review with full code listing].
[20] M.W. Evans and G. Wagnière, Phys. Rev. A 42 (1990) 6732.
[21] M.W. Evans, W.T. Coffey and P. Grigolini, Molecular diffusion (Wiley–Interscience, New York, 1984; MIR, Moscow, 1988).
[22] M.W. Evans and C.R. Pelkie, Visualisation unit of Cornell Theory Center, Ithaca, NY 14853, USA. Thirty minute video with narration, to be published by Farago.
[23] M.W. Evans, G.J. Evans, W.T. Coffey and P. Grigolini, Molecular dynamics (Wiley–Interscience, New York, 1982) ch. 1.
[24] E. Clementi, ed., MOTECC series of volumes (Escom, Leiden).
[25] M.W. Evans, J. Mol. Liq. 32 (1986) 173.
[26] M.W. Evans, G.C. Lie and E. Clementi, J. Chem. Phys. 88 (1988) 5157.
[27] M.W. Evans, G.C. Lie and E. Clementi, Phys. Rev. A 36 (1987) 226; 37 (1988) 2548, 2551.
[28] M.W. Evans, G.C. Lie and E. Clementi, Chem. Phys. Lett. 138 (1987) 149.
[29] D.C. Hanna, M.A. Ťuratich and D. Cotter, Non-linear optics of free atoms and molecules (Springer, Berlin, 1979).